

Available online at www.sciencedirect.com**ScienceDirect**

Energy Procedia 38 (2013) 823 – 832

Energy

Procedia

SiliconPV: March 25-27, 2013, Hamelin, Germany

Passivating properties of hydrogenated amorphous silicon carbide deposited by PECVD technique for photovoltaic applications

Aurélien Gaufres*, Frédéric Husser, Erwann Fourmond, Mustapha Lemiti

Université de Lyon, Institut des Nanotechnologies de Lyon (UMR-CNRS 5270), INSA de LYON, 7 Avenue Jean Capelle, 69621 Villeurbanne Cedex, France

Abstract

Amorphous hydrogenated silicon carbide ($a\text{-SiC}_x\text{:H}$) could be used as a passivating layer in solar cell configuration. We have deposited $a\text{-SiC}_x\text{:H}$ by plasma enhanced CVD on polished silicon wafers. Si-rich $a\text{-SiC}_x\text{:H}$ allows to reach a surface recombination velocity of 7.5 cm.s^{-1} . The hydrogenation of silicon surface dangling bonds and the electrical field-effect near the interface are analyzed by minority carrier lifetime and $C(V)$ measurements and additional FTIR and XPS spectroscopy. The fixed charges within the layers are found to be amphoteric. The interface trap density increases with carbon content in $a\text{-SiC}_x\text{:H}$ because of a lower hydrogen content at the $a\text{-SiC}_x\text{:H}/\text{Si}$ interface. The polarity of the fixed charge is depending on the presence of a metallic contact. As $a\text{-SiC}_x\text{:H}$ may be considered as a semiconductor, the $a\text{-SiC}_x\text{:H}/\text{c-Si}$ interface is in inversion regime at equilibrium inducing a band bending and accumulation when adding a metallic contact.

© 2013 The Authors. Published by Elsevier Ltd. Open access under [CC BY-NC-ND license](#).

Selection and/or peer-review under responsibility of the scientific committee of the SiliconPV 2013 conference

Keywords: silicon carbide, PECVD, passivation, fixed charge, interface traps

1. Introduction

Nowadays, efforts are made to reduce the manufacturing costs and to improve solar cell performances. The thinning of silicon solar cells leads to a greater impact of the surface properties compared to the volume ones. Attention must be thus paid to the surface passivation at the front and the rear side of the solar

* Corresponding author. Tel.: +33-4-72-43-74-62; fax: +33-4-72-43-85-31.

E-mail address: aurelien.gaufres@insa-lyon.fr.

cell. Amorphous hydrogenated silicon carbide (a-SiC_x:H) may be an interesting alternative for the back surface passivation.

The surface passivation properties of a-SiC_x:H deposited by radio-frequency plasma enhanced chemical vapor deposition (RF-PECVD at 13,56 MHz) have been previously reported by I. Martin et al. on a p-type doped [1] and n-doped [2] crystalline silicon substrate. They found a surface recombination velocity which was lower than 30 cm.s⁻¹ on p-type silicon and 54 cm.s⁻¹ on n-type silicon. In ref. [2], the amphoteric nature of the fixed charge within a-SiC_x:H is highlighted.

Our work consisted in optimizing the deposition of a-SiC_x:H for passivation of silicon solar cells, using low frequency PECVD. The layers were then characterized electrically and with minority carrier lifetime measurements. Emphasis is put in the present article on the surface passivation capabilities of a-SiC_x:H.

2. Experiments

a-SiC_x:H layers were deposited on c-Si wafers, Float-Zone quality, (100)-oriented wafers with both n- and p- doping type with a resistivity comprised between 2 to 5 Ω.cm, using a semi-industrial RF-PECVD reactor (440 kHz) from SEMCO Engineering [3]. The samples were cleaned before deposition using CARO chemical cleaning and an HF dip. The temperature of deposition was 370°C, the pressure in the reactor 1500 mTorr and the plasma power density was 0.052 W.cm⁻². Precursor gases were silane (SiH₄) and methane (CH₄). The varying parameter between the samples was the carbon proportion, related to the variation of the precursor gases flow rates, and which is defined as:

$$[C] = \frac{\text{at.\% C}}{\text{at.\% C} + \text{at.\% Si} + \text{at.\% H}} \quad (1)$$

The atomic percentages within the layers were determined by X-Ray Photoelectron spectroscopy measurements (XPS) and Elastic Recoil Detection Analysis (ERDA) for hydrogen. Minority carrier lifetime measurements were made with a Sinton Consulting WCT-100 apparatus using the QSSPC method [4]. Besides minority carrier lifetime, fixed charge density was extracted from the QSSPC measurement, as described in the following section. These data were correlated with values obtained from capacitance-voltage (C(V)) measurements using a mercury-probe contact (Metal/a-SiC_x:H/c-Si structures). Interface trap density was also determined by C(V). This parameter is correlated with the passivation of the interface dangling bonds by Si-H and Si-Si bonds, whose concentration is related to the peak intensity measured by XPS.

3. Analytical description of the surface passivation for parameters extraction

3.1. Parameters extraction from C(V) measurements

We followed a model from Nicollian and Brews [5] to simulate the capacitance-voltage characteristic in case of a Metal-Insulator-Semiconductor (MIS) structure, and to extract the fixed charge density Q_f within the a-SiC_x:H layer. We present here a brief overview of the calculus, which relies on this basic equation:

$$V_G = V_{FB} - \frac{Q_{SC}}{C_I} + \psi_S \quad (2)$$

V_G is the gate voltage, V_{FB} is the flat band voltage, Q_{SC} is the charge density in the c-Si, C_I is the capacitance of the a-SiC_x:H layer and Ψ_S is the surface potential near the c-Si/a-SiC_x:H interface.

The model consists of finding the value of the unknown Ψ_s which satisfies eq. 2. With this equation, a fitting curve can be plotted from which V_{FB} and C_i values are determined. Then Q_f is deduced from the expression of V_{FB} :

$$V_{FB} = \Phi_{ms} - \frac{Q_f}{C_i} \quad (3)$$

where Φ_{ms} is the related metal-semiconductor work difference.

The accuracy of this model is tested with a thermal oxide grown on one of our silicon substrate corresponding to a reference MIS structure for $C(V)$ measurement (figure 1).

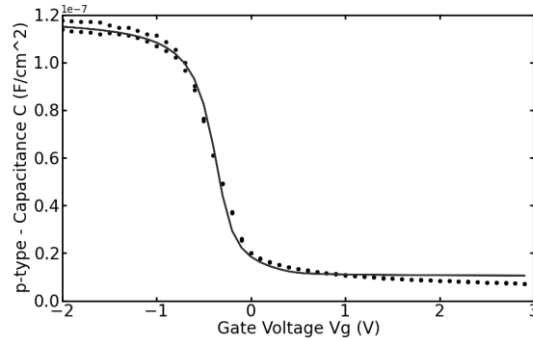


Fig. 1 : Nicollian model fits (solid lines) applied to experimental $C(V)$ curves (dots) of a thermal oxide with a p-type c-Si, measured at a frequency of 1 kHz

The model does not describe precisely the experimental points in the inversion part of $C(V)$ curves. However, the flat band voltage and the oxide capacitance are well described.

3.2. Parameters extraction from QSSPC measurements

The extraction of Q_f from minority-carrier lifetime versus injection rate characteristic is made using the extended Shockley-Read-Hall formalism. Girisch *et al.* [6] have developed a model already used in literature [7], modified [8],[9], and based on an Insulator-Semiconductor (IS) structure, in our case, a single layer of a-SiC_x:H deposited on silicon substrate. The model takes into account the fixed charge density inside the insulator Q_f , the interface charge Q_{it} and the charge inside the semiconductor Q_{sc} . At the equilibrium, these quantities are related following charge neutrality equation:

$$Q_f + Q_{it} + Q_{sc} = 0 \quad (4)$$

According to the hypothesis of Brody *et al.*[9], Q_{it} can be neglected. Q_{sc} is dependent of the quasi-Fermi levels Φ_n and Φ_p and on the surface potential Ψ_s :

$$Q_{sc} = \pm \sqrt{\frac{2kTn_i\epsilon_0\epsilon_{Si}}{q^2}} F(\psi_s, \phi_n, \phi_p) \quad (5)$$

$$\text{with } F(\psi_s, \phi_n, \phi_p) = e^{\frac{q\phi_p}{kT}}(e^{-\psi_s} - 1) + e^{-\frac{q\phi_n}{kT}}(e^{\psi_s} - 1) + \frac{q}{kT}\psi_s \frac{N_A - N_D}{n_i} \quad (6)$$

where all the symbols have their standard meanings. n_b (resp. p_b) are the electron (resp. holes) bulk concentrations and n_i is the intrinsic carrier density. The quasi-Fermi potentials are determined as:

$$\begin{cases} \phi_n = \frac{kT}{q} \ln \left(\frac{n_b + \Delta n}{n_i} \right) \\ \phi_p = \frac{kT}{q} \ln \left(\frac{p_b + \Delta n}{n_i} \right) \end{cases} \quad (7)$$

An initial value of Q_f is introduced in the calculus routine, and Ψ_s is then numerically solved in order to satisfy eq 4. The aim is to fit the experimental lifetime curve ($\tau = f(\Delta n)$) by adjusting the Q_f value. We thus need to describe Shockley-Read-Hall recombinations at the a-SiC_x:H/c-Si interface. From Shockley equations [10], the surface recombination rate U_s is calculated using the fundamental electron and hole recombination velocity (resp. S_{n0} and S_{p0}).

From the previously determined Ψ_s value, the surface carrier densities are defined as :

$$\begin{cases} n_s = n_b e^{\left(\frac{q\psi_s}{kT}\right)} \\ p_s = p_b e^{\left(-\frac{q\psi_s}{kT}\right)} \end{cases} \quad (8)$$

U_s is then expressed with all these parameters as :

$$U_s = \frac{n_s p_s - n_i^2}{n_s + n_i / \frac{S_{p0}}{S_{n0}} + p_s + n_i / \frac{S_{n0}}{S_{p0}}} \quad (9)$$

Finally, the routine is processed again with Q_f , S_{n0} and S_{p0} as fitting parameters until simulated and experimental lifetime curves coincide (see table 1 and 2).

4. Surface passivation in relation with Q_f

To extract the surface recombination rate S_{eff} we use the expression of the effective lifetime τ_{eff} :

$$\frac{1}{\tau_{eff}} = \frac{1}{\tau_b} + \frac{2S_{eff}}{W} \quad (10)$$

where τ_{eff} and τ_b are the effective (resp. bulk) lifetime and W the wafer thickness. The bulk lifetime for the calculation of S_{eff} is set to 6 ms, according to the manufacturer specifications.

In terms of passivation, Si-rich a-SiC_x:H reaches a lifetime at $\Delta n = 10^{15} \text{ cm}^{-3}$ of 1.31 ms on p-type and 949 μs on n-type c-Si, which corresponds to an effective surface recombination velocity of 7.5 cm.s^{-1} and 11 cm.s^{-1} respectively (fig. 2) which is better than values reported in [1] and [2] but lower than doped a-SiC_x:H [11].

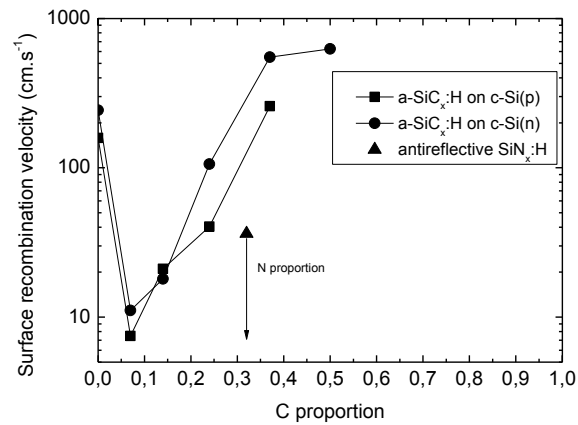


Fig.2. Effective surface recombination velocity for several $[C]$ values. Standard silicon nitride is indicated as a reference.

Fixed charge densities responsible for the field effect passivation were extracted using previous models. The extended SRH model applied to minority carrier lifetime is shown on figure 3 and the curves from Nicollian model applied to $C(V)$ measurements are illustrated on figure 4.

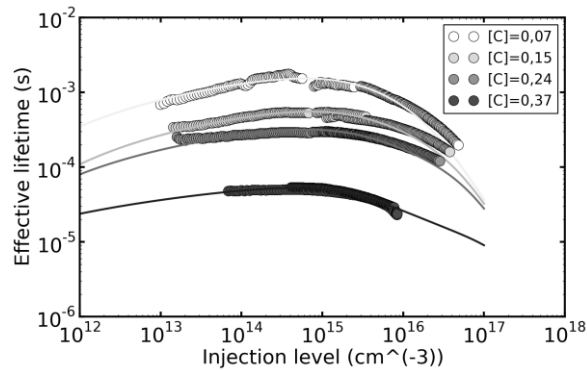


Fig. 3. Results of the extended SRH formalism fit (solid lines) applied to the experimental lifetime curves on p-type substrates (dots).

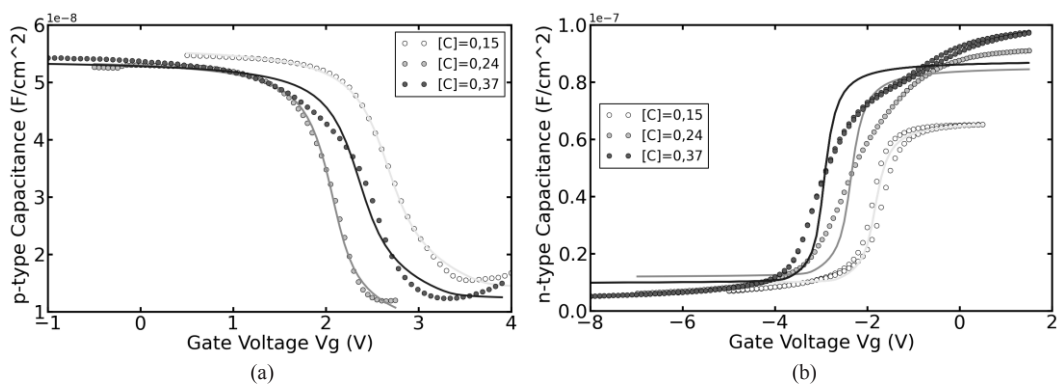


Fig. 4. Nicollian model fits (solid lines) applied to experimental $C(V)$ curves (dots) with an p-type (a) and n-type (b) c-Si, measured at a frequency of 1 kHz.

The Q_f values extracted from lifetime measurements are compared to values obtained from C(V) in Table 1.

Table 1. Q_f concentrations determined by Girisch and Nicollian model.

SDT*	[C]	$Q_f(\text{cm}^{-2})$ (IS** structure) with lifetime curves	$Q_f(\text{cm}^{-2})$ (MIS structure) with Nicollian model
n	0.07	$-6.77 \cdot 10^{10}$	$3.09 \cdot 10^{11}$
n	0.15	$-9.21 \cdot 10^{10}$	$6.79 \cdot 10^{11}$
n	0.24	$-7.92 \cdot 10^{10}$	$1.07 \cdot 10^{12}$
n	0.37	$-1.04 \cdot 10^{11}$	$1.39 \cdot 10^{12}$
p	0.07	$1.16 \cdot 10^{11}$	
p	0.15	$1.20 \cdot 10^{11}$	$-9.16 \cdot 10^{11}$
p	0.24	$1.27 \cdot 10^{11}$	$-7.08 \cdot 10^{11}$
p	0.37	$1.44 \cdot 10^{11}$	$-7.80 \cdot 10^{11}$

* SDT substrate doping type

** IS : Insulator – Semi-conductor

When comparing Q_f values, we have to remember that the measurement conditions are different between the two cases. The lifetime curves are obtained by QSSPC measurements without any electrical contact on a single a-SiC_x:H layer deposited on the silicon substrate. The C-V curves corresponds to a MIS structure with a metallic contact on the a-SiC_x:H layer.

Table 2. Fundamental velocity of electrons S_{n0} and holes S_{p0} determined by Girisch model.

SDT	[C]	$S_{n0}(\text{cm.s}^{-1})$	$S_{p0}(\text{cm.s}^{-1})$
n	0.07	53	51,4
n	0.15	277	55,3
n	0.24	910	229
n	0.37	8780	410
p	0.07	18,7	64,8
p	0.15	29,5	205
p	0.24	53,6	405
p	0.37	2360	3130

From the lifetime curves fit, the fixed charge density is negative in case of n-type c-Si substrate and positive in case of p-type c-Si substrate (table 1). The defects related to fixed charge density is therefore amphoteric, as reported by I. Martin [2]. For n-type silicon, higher S_{n0} values (table 2) means that electrons recombine more rapidly in positively charged defects. Since the interface is in inversion regime, holes are the majority carrier. The passivation is governed by S_{p0} values. The situation is symmetrical in the case of p-type silicon with values of S_{n0} .

Moreover, we note that the Q_f sign for each sample is opposite when comparing the values extracted from lifetime curves and those from C(V) curves (table 1). Besides the point that the metal coverage changes the measurement conditions, further explanation will be given on the discussion part (see figure 7).

A major information is finally that the absolute fixed charge density increases as [C] increases. We also note that the fixed charge density calculated from the n-type silicon C(V) measurement is generally one order of magnitude above the values determined by the extended SRH model. We had difficulties to complete C(V) measurements with a-SiC_x:H layers, especially for n-type substrate. Important leakage currents were observed by I-V measurements, which induced a strong increase of the capacitance inside the measured voltage range.

5. Characterization of the interface traps

Silicon dangling bonds which are present at the surface of the silicon substrate corresponds to additional electrical traps for the photogenerated carriers in the bandgap. The interface trap density noted D_{it} is derived from the comparison between the experimental and simulated C-V curves using the Terman model [12]. The voltage difference is related to Q_{it} and using the surface potential Ψ_s , the model can draw the repartition of the interface traps within the bandgap. E_s is the varying energy level during measurement and E_f is the Fermi level (figure 5).

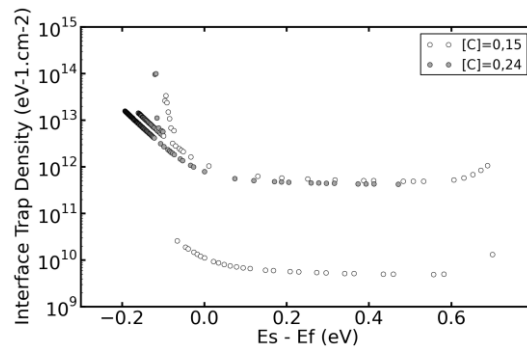


Fig. 5. Interface trap density vs energy level in the bandgap obtained with the application of Terman method to an p-type sample. Note the increase of D_{it} close to $E_s - E_f = -0.1$ eV.

Extraction of D_{it} is made difficult due to the importance of the leakage current which introduces some noise in C(V) measurements, as already mentioned. We note however the increase of density of defects from about 10^{10} to 10^{12} eV⁻¹.cm⁻² between $[C]=0.15$ and $[C] = 0.24$. This increase is in fact attributed to the less passivating film (fig. 2).

Attention is paid to Si-Si and Si-H bonds concentration within the layers, as they are responsible for filling in the silicon surface dangling bonds and, consequently, for the passivation. From XPS and FTIR measurements, we obtained the following values of Si-H and Si-Si bonding absorptions related to bonding concentrations inside the a-SiC_x:H layer for each samples :

Table 3. Si-H and Si-Si bonding peak intensity for each samples

[C]	peak intensity of Si-H + Si-Si bonds (a.u.) (from XPS measurements)	peak intensity of Si-H bonds (a.u.) (from FTIR measurements)
0.07	27553	174
0.15	7681	102
0.37	7525	60

The Si-H and Si-Si bonding concentrations decrease with the carbon content and are also related to the increase of the surface recombination velocity (fig. 2). The decrease of Si-Si and Si-H bonds within the a-SiC_x:H layers can thus be related to a decrease of these bonds at the interface. This is in agreement with the small increase of D_{it} between $[C] = 0.15$ and $[C] = 0.24$ (fig. 5).

6. Discussion and conclusion

Si-rich $a\text{-SiC}_x\text{:H}$ is a good passivating layer with a minimum surface recombination velocity of 7.5 cm.s^{-1} . This passivation is partly achieved the completion of silicon dangling bonds at the interface with H and/or Si, leading to a decrease of the interface trap density D_{it} . The field effect due to fixed charge Q_f within the layer plays also a role in the passivation.

When carbon content increases within the layer, the Si-H bonds decreases and entails a degradation of D_{it} . The sign of the extracted fixed charge was found to be opposite when comparing the lifetimes curves and the $C(V)$ curves. We also notice that the Nicollian fit does not converge perfectly with the experiment. This could be related to current leakage and surface states. $a\text{-SiC}_x\text{:H}$ is in fact known to be a difficult material for capacitance-voltage measurements, since it is a weak insulator, contrary to other dielectrics like SiO_2 or $\text{SiN}_x\text{:H}$. Then, we have to consider the fixed charges and the interface charges related to the defects in $C(V)$ measurements. The optical bandgap of our samples, as determined by optical analysis, varies in fact from 1.8 to 2.3 eV.

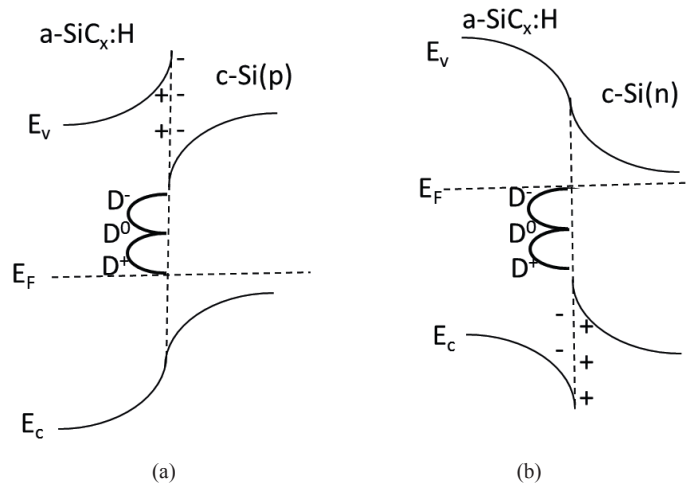


Fig. 6. Band diagram drawing of $a\text{-SiC}_x\text{:H}/c\text{-Si}$ interface at equilibrium for p- (a) and n-type (b) silicon (representation of interfacial defects in $a\text{-SiC}_x\text{:H}$ are represented as described for $a\text{-Si:H}$ in Olibet et al. [13]). Work function of $a\text{-SiC}_x\text{:H}$ is estimated lower than $c\text{-Si}$.

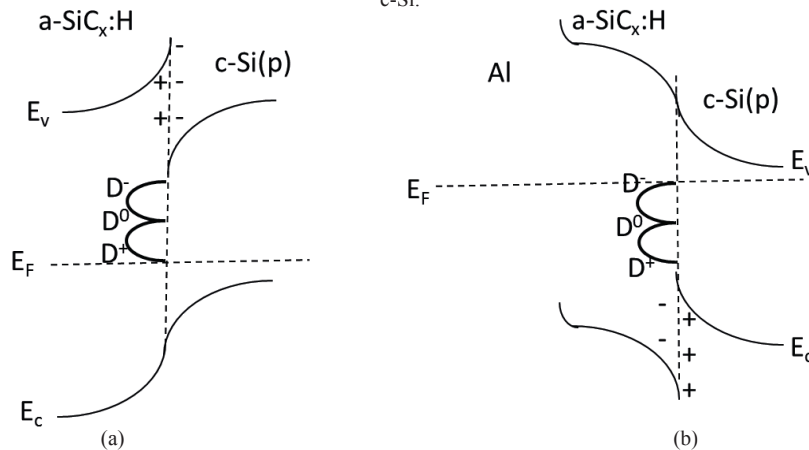


Fig. 7. Evolution of the $a\text{-SiC}_x\text{:H}/c\text{-Si}$ band diagram without (a) and with (b) a metallic contact

Without aluminum contact (fig. 6), Q_f values (table 1) shows that there is an inversion regime at the interface, with a-SiC_x:H/c-Si structure. The resulting band bending at the interface induces a shift of the Fermi level. This leads to a change on the polarity of the charged defect at the interface. When connecting the aluminum contact, the alignment of Fermi levels of Al/a-SiC_x:H/c-Si structure is different. This induces a shift of the Fermi level in a-SiC_x:H bandgap (fig. 7). The energy distribution of defects is then shifted from above to below the Fermi level. Finally, the situation is characteristic of an accumulation regime.

The MIS configuration used for C(V) also seems to be a limiting model since the band offsets between a-SiC_x:H and c-Si are relatively low (about 0.44 – 1 eV) as reported in [14] and a-SiC_x:H seems to be more a semiconductor than a dielectric. Charges transfer may thus happen between a-SiC_x:H and c-Si.

The extended SRH formalism for lifetime fit is based on the hypothesis that the interface states are negligible as for SiN_x:H or SiO₂. But in figure 5 from Terman model, we observe that this hypothesis is not automatically suitable for a-SiC_x:H. The values of the parameters describing the lifetime curves fitting model are also physically reliable and in agreement with the literature [2][7].

However the sign of the flat-band voltage extracted from C(V) curves (fig. 4) is determined without any ambiguity and the change of sign between n-type silicon substrate and p-type silicon substrate is clear. Considering the fixed charge density and the interface charge, the Al/a-SiC_x:H/c-Si structure stands thus in accumulation regime independently on the doping type of the substrate.,

The use of a-SiC_x:H as a rear-side passivating layer is considered in an industrial solar cell scheme as it has been done by Suwito et al. [15]. This will be the object of a next publication.

Acknowledgements

I would like to acknowledge Nanolyon Platform team who took a certain part in this work. Funding is provided by a grant from Région Rhône-Alpes (France).

References

- [1] I. Martin, M. Vetter, A. Orpella, J. Puigdollers, A. Cuevas and R. Alcubilla, *Applied Physics Letters*, vol. 79, no. 14, pp. 2199–2201, 2001.
- [2] I. Martin, M. Vetter, A. Orpella, C. Voz, J. Puigdollers and R. Alcubilla, *Applied Physics Letters*, vol. 81, no. 23, pp. 4461–4463, 2002.
- [3] J. Dupuis, E. Fourmond, D. Ballutaud, N. Bererd and M. Lemiti, *Thin Solid Films*, vol. 519, no. 4, pp. 1325–1333, 2010.
- [4] R. A. Sinton, *Applied Physics Letters*, vol. 69, no. 17, pp. 2510–2512, 1996.
- [5] E. H. Nicollian and J. R. Brews, *MOS Physics and Technology*, Wiley-Inte. 1982.
- [6] R. B. M. Girisch, R. P. Mertens and R. F. De Keersmaecker, *IEEE Transactions on Electron Devices*, vol. 35, no. 2, pp. 203–222, 1988.
- [7] I. Martín, M. Vetter, M. Garín, A. Orpella, C. Voz, J. Puigdollers and R. Alcubilla, *Journal of Applied Physics*, vol. 98, no. 11, p. 114912, 2005.
- [8] A. G. Aberle, S. Glunz and W. Warta, *Journal of Applied Physics*, vol. 71, pp. 4422–4431, 1992.
- [9] J. Brody and A. Rohatgi, *Solid-State Electronics*, vol. 45, no. 9, pp. 1549–1557, Sep. 2001.
- [10] W. Shockley and W.T. Read Jr. *Physical Review B*, vol. 87, no. 5, pp. 835–842, 1952.
- [11] S. Janz, S. Riepe, M. Hofmann, S. Reber and S. Glunz, *Applied Physics Letters*, vol. 88, no.13, p. 133516, 2006
- [12] L. M. Terman, *Solid-State Electronics*, vol. 5, no. 5, pp. 285–299, 1962.
- [13] S. Olibet, E. Vallat-Sauvain, C. Balif, *Physical Review B*, vol. 76, p 35326, 2007

- [14] T. M. Brown, C. Bittencourt, M. Sebastiani and F. Evangelisti, *Physical Review B*, vol. 55, no. 15, pp. 9904–9909, 1997
- [15] D. Suwito, U. Jäger, J. Benick, S. Janz, M. Hermle, R. Preu, S.W. Glunz, *25th European Photovoltaic Solar Energy Conference*, 2010, pp. 1443–1445